Fracture Toughness and Fracture Energy, Mihashi et al. (eds)
© 1989 Balkema, Rotterdam. ISBN 90 6191 988 6

A novel testing technique for post-peak tensile behavior of cementitious materials

Victor C.Li & Robert J.Ward
Massachusetts Institute of Technology, Cambridge, Mass., USA

ABSTRACT: A novel technique based on the J-integral is employed to experimentally determine the tension-softening (σ–δ) relations in cementitious composites. The σ–δ relation provides information on fracture resistance and could be used for numerical simulations of crack formation and propagation in structures constructed from materials which exhibit tension-softening behavior. The present method requires no complicated modifications of testing machines. In the experiment, pre-notched specimens with slightly different notch lengths are used. The corresponding values of load, load point displacement and crack tip separation are simultaneously recorded. From these experimental data, the J-integral as a function of crack tip separation as well as the tension-softening curve can be deduced. These curves also provide a measure of the critical energy release rate and hence fracture toughness of the tested material. The experimental technique has been verified numerically for both the compact tension configuration and for the 4-point bend beam configuration. Applications of this test method to plain mortar, and mortar reinforced by steel, acrylic and Kevlar fibers have been performed and found to provide reasonable results. Limited comparisons with test results from direct tension test method and the RILEM-recommended G_F-fracture test method are also presented. A summary of the current status of the J-based test method is included.

1 INTRODUCTION

Concrete is used worldwide as a structural material. Due to its low tensile strength and susceptibility to cracking designers have conventionally assumed zero tensile strength and have just used the compressive strength as a basis for design. However, the realization that tensile properties play a key role in the phenomena such as shear punching, bond crack resistance and size effect have led to dramatically increased research in this area in recent years.

Strength and ductility are two very desirable properties of a structural material. It is generally agreed however, that as the strength of a cement-based material is increased, its ductility decreases. Recently, very high strength concretes have been produced by the addition of silica fume, fly-ash or superplasticizer to the cement matrix or by pressure application after casting. 130 MPa concrete (almost four times as strong as conventional concrete) has been used on Seattle's Two Union Square building. This development raises the question of how brittle is this almost new material compared to conventional concrete and how will it behave when subjected to stresses which are not purely compressive.

Experience has shown that the failure stress of concrete structures shows a general decrease as structural size is increased. Also, larger structures tend to be characterized by more sudden and energy-packed failures. Most design codes have not accounted for this phenomenon because of the lack of an adequate explanation for it.

Fiber reinforced concrete is generally distinguished from plain concrete, not by any significant change in tensile strength, but rather by its ability to absorb much larger amounts of energy, its greater resistance to crack propagation, its ability to withstand large deformations and its overall ductility. This distinction is not adequately reflected in conventional test data such as a pre-peak stress-strain curve.

A common thread connecting the above mentioned phenomena is that, while conventional "strength" theories fail to provide adequate explanations, a fracture mechanics approach is useful in each case. Fracture mechanics relies on a very important material characteristic generally known as fracture resistance. When attempting to define fracture resistance it is necessary to have some understanding of the physical processes which lead to fracture in a material such as concrete. When loaded in tension the material follows a stress-strain curve up to the maximum load at which point the deformation localizes onto an eventual fracture plane. Once a macroscopic crack has formed microcracking in the cement paste and in the cement-aggregate interface as well as aggregate and fiber pull out where applicable dissipate the energy which is responsible for the propagation of the macrocrack. This zone of inelastic deformation, often referred to as the process zone, appears to be rather planer on the macroscopic scale. If this deformation at the crack tip is confined to a small region (relative to the crack size and the specimen dimensions) and if the material outside the process zone behaves elastically, then it is possible to use LEFM. In such a case the fracture toughness K_{IC} could be used as a measure of fracture resistance and the energy release rate G_c could be found from $G_c = K_{IC}^2/E$. However it is very unlikely that cracking in concrete obeys the LEFM assumptions unless the specimen is very large. Hillerborg (1983) shows that for 3-point bend specimens, beam depths of less than 1-2 m would give invalid K_{IC} results. K_{IC} values obtained from tests on laboratory sized specimens show some kind of size dependence with larger values obtained for large size specimens. Thus it is not normally possible to use a laboratory measured K_{IC} value as a fracture resistance parameter which is a true material property. For this reason it is necessary to look outside LEFM for a measure of fracture resistance which depends only on the material. The constitutive relationship between the tensile stress transferred across a crack plane and the separation distance of the crack faces, generally known as the tension-softening (σ–δ) curve is a material property. A number of parameters may be calculated from this curve. The maximum stress value is the tensile strength, f_t, the maximum separation distance is the critical crack opening, δ_c, at which a real crack is formed and the area enclosed by the curve represents the energy required to create a unit area traction-free crack.

The σ–δ curve may be obtained from a direct tension test. However, an inherent difficulty associated with the test is that the deformation is unstable unless a very stiff testing machine is used which is not available in most laboratories. Successful tests have been performed using mechanisms such as parallel steel bars in the direction of loading and closed loop feedback systems by Petersson (1981), Gopalaratnam and Shah (1985), and Reinhardt (1984). Despite this, the rather intricate modifications required prevent this from becoming a standard testing procedure. This paper reviews an indirect J-integral technique which has been used by Li and co-workers (1985), (1987), Leung and Li (1988), and Ward et al (1988) to experimentally determine the σ–δ curve and which requires only an ordinary testing machine and a simple testing procedure. These are important characteristics of any test method which is to be universally adopted. A σ–δ curve for Kevlar reinforced mortar is deduced by this indirect method and a comparison is given with a curve obtained from a direct tension test. Other deduced curves for plain mortar and mortar reinforced with steel and acrylic fibers are described. Also some refinements of both the experimental procedure and the data analysis are suggested which are expected to lead to greater accuracy in the deduced tension-softening curve.

2 THEORETICAL BASIS OF J-INTEGRAL TECHNIQUE

The path independent J-integral is defined as:

$$(1) \quad J = \int_{\Gamma} \left(W dy - \underset{\sim}{T} \frac{\partial \underset{\sim}{u}}{\partial x} ds \right)$$

where Γ is a curve surrounding the notch tip, W is the strain energy density, $\underset{\sim}{T}$ is the traction vector in the direction of the outward normal along Γ, $\underset{\sim}{u}$ is the displacement vector and ds is an arc along Γ. From Eq. (1) Rice (1968a, 1968b) produced two alternative definitions of J. He used the Barrenblatt approach which considers a cohesive zone ahead of the crack tip in which the restraining stress σ(δ) is viewed as a function of separation δ. If the J-integral is evaluated along a contour Γ_1, shown in Fig. 1, which runs along beside the cohesive zone, then we get

$$(2) \quad J = \int_{\substack{\text{cohesive} \\ \text{zone}}} \sigma(\delta) \frac{d\delta}{dx} dx$$

This definition may be interpreted as follows. If the crack opening at each point in the cohesive zone increases by an amount dδ then the profile of the cohesive zone boundary extends a distance dx. The quantity σ(δ)dx is the force over each infinitesimal area and σ(δ) dx dδ is the energy absorbed during increased separation dδ. Thus Eq. (2) defines J as the rate of energy absorption with respect to cohesive zone propagation. Eq. (2) may also be expressed as

$$(3) \quad J = \int_0^{\delta_t} \sigma(\delta)\, d\delta$$

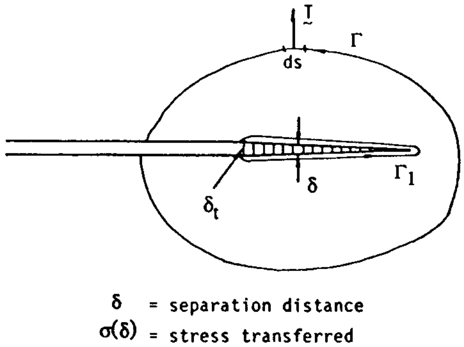

Fig. 1 Cohesive zone ahead of the crack tip.

where δ_t is the separation distance at the crack tip. When δ_t reaches δ_c the real crack propagates and a critical J-integral value, J_c is reached

$$(4)\quad J_c = \int_0^{\delta_c} \sigma(\delta)\, d\delta$$

J_c is equal to the total area under the σ–δ curve and may be interpreted as the rate of energy absorption in the cohesive zone with respect to crack tip propagation.

The second interpretation of J (Rice, 1968) may be given as:

$$(5)\quad J = -\frac{\partial(PE)}{\partial a}$$

where PE is the potential energy of a body with crack length a. Thus J is equal to the rate at which the potential energy of a cracked specimen decreases as the crack propagates.

The basis of our indirect J-integral technique of finding the σ–δ relationship is to find J experimentally using Eq. (5) and then to substitute into Eq. (3) and find $\sigma(\delta)$. Potential energy may be calculated simply from a load-displacement curve. However, since the crack tip position is difficult to locate accurately, it would be almost impossible to directly evaluate Eq. (5) by propagating a crack in a single specimen. One approximate procedure for getting around this problem is to use two cracked specimens identical in every respect except that there is a slight difference in their initial crack lengths. If the load-load point displacement (P-Δ) curves are measured for each specimen, then the area $A(\Delta)$ between the two curves up to a load point displacement Δ represents the difference in energy and Eq. (5) may be interpreted as:

$$(6)\quad J(\Delta) = \frac{A(\Delta)}{B(\Delta a)}$$

where Δa is the difference in crack lengths and B is the specimen thickness. If, during the experiment, the crack tip separation, δ, is also measured then it is possible using the Δ–δ relationship to convert $J(\Delta)$ to $J(\delta)$. Differentiation of Eq. (3) then gives

$$\sigma(\delta) = \frac{\partial J(\delta)}{\partial \delta} \quad (7)$$

and the tension-softening curve may be determined from the slope of the $J(\delta)$ curve.

3 NUMERICAL VERIFICATION OF TEST TECHNIQUE

This method has been verified numerically for both beam bending and compact tension configurations. A. Hillerborg (private communications, 1985) provided verification by employing his fictitious crack model in a finite element scheme to simulate the load-load point displacement curves and load-crack tip separation curves of a pair of three-point bend specimens of slightly different crack lengths. He used an artificial bi-linear curve as input for the tension-softening behavior in the material ahead of the crack tips. The objective of the exercise was to extract the same curve using the indirect J-integral technique with his numerically derived 'test results'. The extracted curve essentially overlapped the initial assumed curve, thus verifying the theoretical basis. Reyes (1987) used a boundary element method to carry out a similar procedure with a compact tension configuration. Again the input curve and the extracted curve showed excellent agreement.

The theoretical basis and numerical verification confirm that this test technique is independent of specimen geometry and should also be independent of specimen size. The only restriction on specimen size is that the smallest specimen dimensions should be a number of times larger (maybe four or five times) than the largest single particles in the material. Thus minimum dimensions depend on material properties such as aggregate size and fiber length.

4 EXPERIMENTAL RESULTS

This technique has been used with both the compact tension and the four-point bend beam configuration shown in Fig. 2. In order to

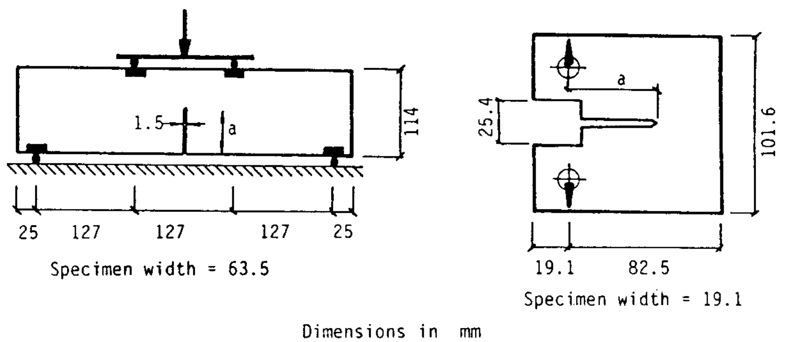

Fig. 2. Specimen configurations used with J-integral test

demonstrate the mechanics of the method, a set of experimental results is given and the deduced tension-softening curve is compared with a curve obtained from a direct tension test. The material used is fiber-reinforced mortar with a water : cement : sand ratio of 0.5 : 1 : 1 and containing two percent by volume of 6.35 mm Kevlar 49 fibers. The use of fibers ensured that it was relatively easy to obtain a stable direct tension test result. The four-point bend beam configuration was used with a short crack length, a_1 equal to 57.15 mm and a long crack length, a_2 equal to 63.5 mm. The notches were cut with a 1.5 mm thick diamond blade, one day before testing. Crack guides, 6.35 mm deep, were cut on each side of the beam so as to confine the propagating crack to a vertical plane ensuring Mode I fracture. Without these crack guides, the crack may sometimes deviate quite considerably from a vertical path especially when fibers are present in the material. As a preliminary investigation into the behavior of this composite only two beams were tested for each crack length compared to a usual minimum of four.

Fig. 3 shows the average load versus load point displacement curves for each crack length. Fig. 4 shows three different average crack

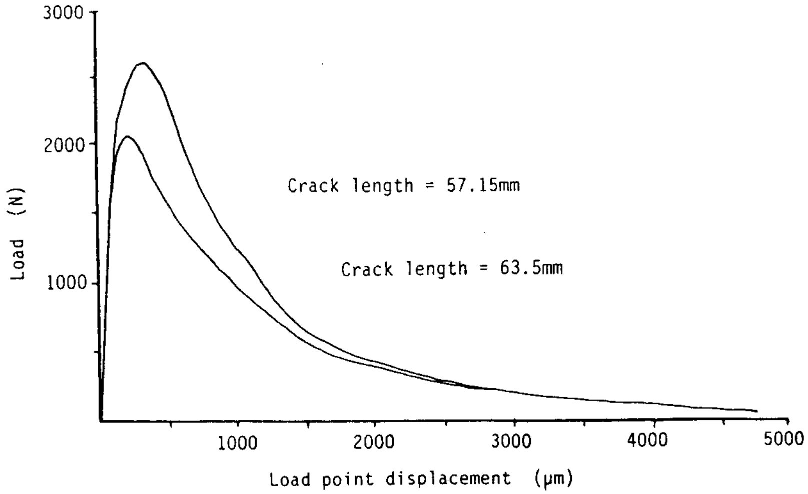

Fig. 3. Average load versus load point displacement curves.

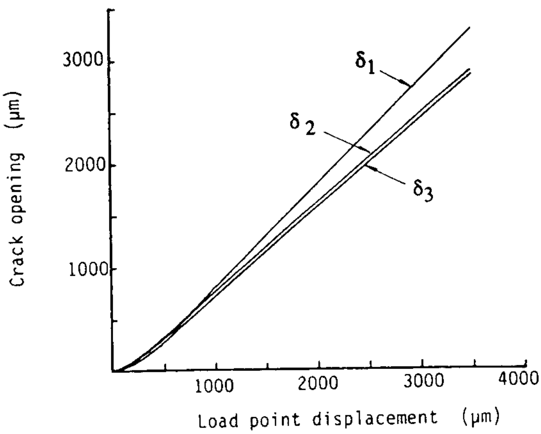

Fig. 4. Load point displacement versus crack opening curves.

opening values, δ_1, δ_2, and δ_3 , expressed as a function of load point displacement. δ_1 was measured at the initial crack tip of the short cracked beams, δ_2 at the initial crack tip of the long cracked beams, and δ_3 at a point 6.35 mm (equal to Δa) above the crack tip in the short cracked beams. Previous experimental programs have used $\delta = (\delta_1 + \delta_2)/2$ as the average crack opening value. Closer examination of the experimental procedure indicated that the use of δ_3 in place of δ_2 may be more correct. From Fig. 4 it may be observed that by using $\delta = (\delta_1 + \delta_3)/2$ instead of the previous definition, the deduced stress is higher for the initial part of the σ–δ curve and lower over the central part. As will be seen later, this leads to an improvement in the accuracy of the deduced curve. More tests are required to establish the best definition of δ. Using numerical integration, a J-Δ relationship was calculated as shown in Fig. 5. Numerical differentiation of the J-δ curve was achieved using Taylor expansions at five consecutive points $J(\delta-g)$, $J(\delta-h)$, $J(\delta)$, $J(\delta+j)$, $J(\delta+k)$ and solving for $J'(\delta)$. Fig. 6 shows the deduced tension-softening curve. It shows an initial rise from $\sigma=0$ to $\sigma=f_t$

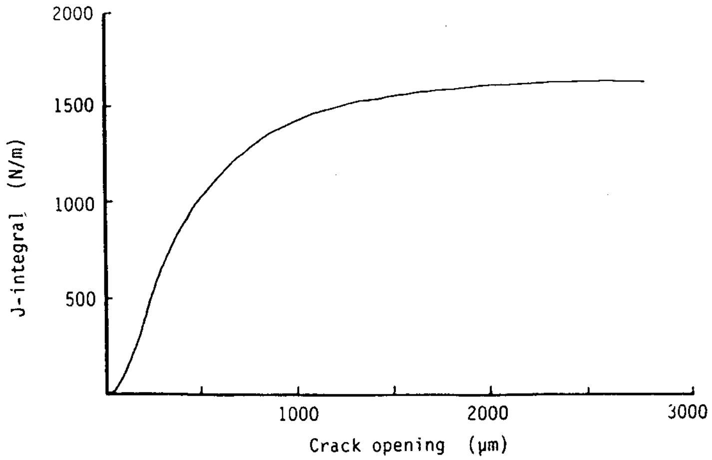

Fig. 5. J-integral versus crack opening curve.

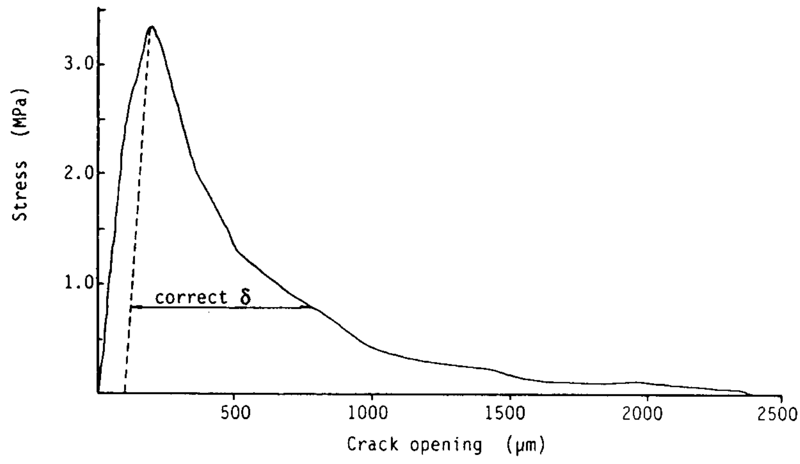

Fig. 6. Deduced tension softening curve.

before descending back down to σ=0. This initial ascending part may be interpreted as the sum of recoverable elastic deformation and inelastic deformation caused by microcracking prior to the localization of deformation onto the fracture process zone and therefore should not be regarded as part of the σ–δ relationship. Figure 7 shows the corrected σ–δ curve as well as the curve obtained from the direct tension test. Considering the limited number of

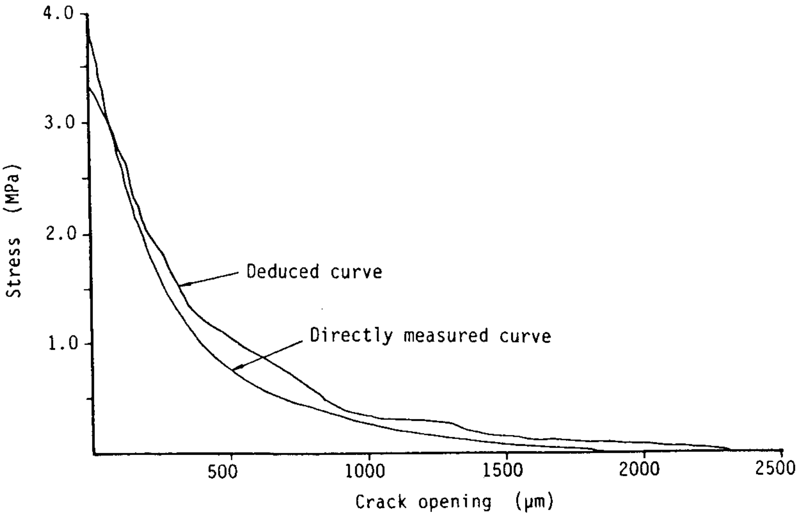

Fig. 7. Comparison between directly measured and deduced tension-softening curves.

tests carried out, the agreement is reasonably good. The deduced tensile strength is 3.35 MPa compared to a directly measured value of 3.95 MPa. This underestimation is consistent with previous test results and some explanation for it as well as some refinements which may reduce the error are discussed in the next section. The critical J-integral value, J_c, is 1485 N/m com- pared to the directly measured value of 1250 N/m. This error can be attributed mainly to the small number of tests and could be largely eliminated by carrying out four or five tests for each crack length. Fracture energy was also calculated in accordance with the RILEM-recommended G_F method using the curves in Fig. 3 and G_F defined as:

$$(8)\quad G_F = \frac{A}{B(d-a)}$$

where A is the total area under the load versus load point displacement curve including an approximate correction for energy supplied by the self-weight of the beam as proposed by Petersson (1981) and d is the overall beam depth. The calculated values were 1181 N/m and 1143 N/m for the short crack and long crack beams respectively. These G_F values are less than the energy value obtained from the direct test and this observation is the opposite of test results obtained by Horvath and Persson (1984) who found G_F values to be about 20% greater than direct tension results. Their tests were carried out on plain concrete specimens in which the maximum beam deflections were of the order of 1 mm. In our tests maximum recorded beam deflections were of the order of 5 mm with a very long flat tail on the load-displacement curves. The self-weight correction method attempts to estimate the area which would lie under this long tail if the beam did not fail under self-weight and the load gradually decreased to zero. It is possible that the correction applied to plain concrete which has a relatively short tail is not directly applicable to fiber reinforced concrete which has a much longer tail. This may account for differences in the observed trend when comparing plain and fiber reinforced concrete.

5 SUMMARY OF EXPERIMENTAL WORK

Initially a brief description is given of the various materials which have been tested to date followed by a summary of the J-integral test results.

Material #1 is mortar with a water : cement : sand ratio of 0.5 : 1 : 2. The compact tension configuration shown in Fig. 2 was used with initial crack lengths of 35.56 mm and 43.18 mm. Four specimens were tested for each crack length at seven days.

Material #2 is steel fiber reinforced mortar with a water : cement : sand ratio of 0.5 : 1 : 2 and a fiber volume fraction of one percent. The fibers had length 9.525 mm and effective diameter 0.1524 mm. The beam bending configuration shown in Fig. 2 was used with initial crack lengths of 44.45 mm and 54.61 mm. 5.1 mm crack guides were used. Four specimens were tested for each crack length at seven days.

Material #3 is acrylic fiber reinforced mortar with a water : cement : sand ratio of 0.8 : 1 : 2 and a fiber volume fraction of one percent. The fibers had length 12.7 mm and diameter 14.2 μm. The beam bending configuration was used with initial crack lengths of 42 mm and 50.5 mm. Eight specimens were tested for each crack length at seven days.

Material #4 is mortar with a water : cement : sand ratio of 0.5 : 1 : 1. The beam bending configuration was used with initial crack lengths of 42 mm and 50.5 mm. Eight specimens were tested for each crack length at fourteen days.

Material #5 is similar to #4 except that a one percent volume fraction of 6.35 mm long and 13.6 μm diameter acrylic fibers are added.

Material #6 is similar to #5 except that the fiber volume fraction is two percent.

Material #7 is similar to #5 except that the fiber volume fraction is three percent.

Material #8 is the Kevlar fiber reinforced mortar described in the previous section.

All the test results are summarized in Table 1 and the deduced tension-softening curves are in Fig. 8. There is good agreement between J_C and G_F but the deduced tensile strength tends to be less than the actual strength. A possible explanation for this tendency is as follows. This J-integral method examines a portion of the crack plane which extends a distance Δa between the positions of the short and long crack tips. The deduced σ–δ curve represents the average stress transferred across this area as a function of the average crack separation. The loading configuration ensures that at any given time during the test the actual crack opening at any point

Table 1. Summary of J-Integral Test Results

Material*	No. of Tests	Deduced f_t (MPa)	J_c (N/m)	δ_c (mm)	Direct f_t (MPa)	G_F (N/m)
1. mortar	4	2.09	84	140	--	--
2. steel FRC	4	2.80	1200	3700	3.0	--
3. acrylic FRC	8	1.78	187	700	--	--
4. mortar	8	2.09	81	190	2.6	78
5. acrylic FRC	8	2.08	205	1100	2.6	209
6. acrylic FRC	8	2.01	404	1520	2.6	414
7. acrylic FRC	8	2.11	543	1340	2.6	607
8. kevlar FRC	2	3.35	1485	2300	4.0	1162

*For mix and fiber volume fraction and length, see text for details.

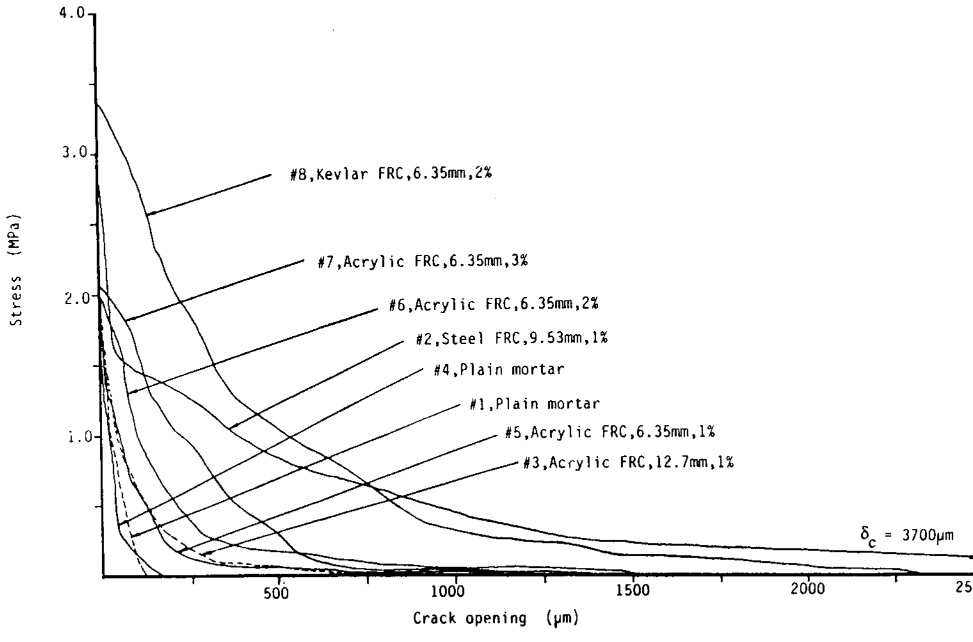

Fig. 8. Tension-softening curves deduced by indirect J-integral techn

within the specified zone gets smaller as the point moves from the initial crack tip towards the neutral axis. When the Δa zone is transferring maximum load, the stress along some line within the zone is equal to the tensile strength. At all other points the stress transferred must be less than f_t. Thus when the average stress throughout the zone is calculated, it must be less than f_t. Theoretically this problem is solved by letting Δa approach zero. In practice, however, there is a lower limit on Δa so that errors in the measurement of initial crack lengths and in the loading machine and instrumentation are not significant. In addition, Δa cannot be too small so that the assumption of a representative homogeneous material for which the averaged mechanical property is being measured is not violated. Experience suggests a lower limit of about 6 mm for the beam bending configuration in Fig. 2. A possible extension of the approach to date may be to use different Δa values in a given test program and to extrapolate the J-δ or the σ-δ curve to obtain a curve as $\Delta a \rightarrow 0$. A variation of this possibility may be to use similar Δa values, to vary the ratio $\Delta a/(d-a)$, and to extrapolate the resulting curves to find a solution as this ratio approaches zero. The problem with these approaches is that the number of test specimens required is considerably increased.

Another source of error in the final result is from the raw data curves. Because this technique relies on measuring the difference between two load versus load point displacement curves obtained from cracked specimens with only a small difference in initial crack lengths, any error in the measured curves results in a magnified error in the difference between the curves. Concrete, and especially fiber reinforced concrete, is a heterogeneous material and so there is always some variation in test results obtained from supposedly exactly similar specimens. In order to guard against the possibility that a single exceptional test result may significantly affect the final deduced tension-softening curve, a standardized approach has been adopted for examining individual raw data curves and combining them to produce average curves which are likely to give a good result. Using each load versus load point displacement curve, two values are calculated, namely G_F and f_f(net) where G_F is as defined in Eq. (5) and f_f(net) is defined as:

$$(9) \quad f_f(\text{net}) = \frac{6M(\max)}{B(d-a)^2}$$

where M(max) is the maximum bending moment resisted by the notched section. It is reasonable to expect that these values are similar for the short cracked and long cracked beams. Thus it is also reasonable to assume that if the raw data curves for each crack length are chosen in a manner which ensures that the two average curves have similar G_F and f_f(net) values, then they are likely to produce an accurate tension-softening curve. The f_f(net) values significantly affect the deduced tensile strength and there is a direct relationship between the two G_F values and the J_c value. This approach is especially useful when the number of tests performed is small.

6 CONCLUSION

As the importance of fracture mechanics and in particular the importance of the tension-softening relationship in the analysis of the structural behavior of a brittle material such as concrete is more widely accepted, it will be imperative that a standard test procedure to determine this relationship exists, which is relatively simple to perform, requires only normal laboratory equipment and is numerically verifiable. Such a testing method is presented here in the form of an indirect J-integral technique and results obtained from tests on Kevlar fiber reinforced mortar compare well with direct tension test results. A set of deduced tension-softening curves, obtained by this method, for plain mortar, and mortar reinforced with steel and acrylic fibers show reasonable agreement with measured tensile strength and G_F values. With some further refinements of the technique, to improve accuracy, this test could become a practical means of obtaining important fracture parameters for tension-softening materials.

7 SUMMARY OF THE CURRENT STATUS OF THE J-BASED TEST METHOD

The J-based test method has undergone extensive development in the last few years, both at MIT and elsewhere. It has been applied to a diverse group of materials, and on specimens of various geometries. The following is a summary of the current status of this test method. It is expected that further developments will have been made by the time this article is published, as several groups in Europe, Japan and in the United States are conducting research in the J-based test method and its applications.

- The J-based test method provides a complete tension-softening curve in addition to the fracture energy. The complete tension-softening curve may be used as a constitutive law beyond the linear stress-strain deformation in computational codes for simulating or predicting concrete structural behavior [Hillerborg (1983)].
- The J-based test method has been applied to an increasingly wide range of materials, including mortar [Li et al (1987)], steel FRC [Leung and Li (1988)] and synthetic FRC (this study), and granite [Hashida (1989)] and basaltic rocks [Chong et al (1989)]. The results have been quite satisfactory.
- The J-based test method is flexible in allowing the use of specimens with various geometries. For example, compact tension specimens have been used by Li et al (1987) and Hashida (1989), 4-point bend beam specimens have been used in this study, semi-circular specimen from rock cores has been used by Chong et al (1989).
- The J-based test method does not require sophisticated or modified loading machines, and is therefore quite suitable for industrial adoption.
- The J-based test method has been verified numerically for two specimen geometries: 3-point beam bending geometry by Hillerborg (personal communications, 1985) using the finite element method; and compact tension geometry by Reyes (1987) using the boundary element method.
- The J-based test method has been successfully applied to specimens which can be much smaller than that required by classical fracture toughness test imposed by LEFM small scale yielding conditions.
- The J-based test method has produced tension-softening curves for mortar [Li et al (1987)], FRC (Li and Ward, this study) and rock [Hashida (1989)] which compares well with data obtained from direct tension tests.
- The J-based test method has produced fracture toughness in a fine grain basaltic rock which compares well with classical fracture toughness test using a very large specimen (9-inch diameter) [Chong et al (1989)].
- The J-based test method has produced fracture energy values for FRC which compares well with that measured using the G_F test technique currently recommended by RILEM (This study).

• The J-based test method has produced limited evidence of size-independence in a study of 3 different specimen sizes in granitic rock [Hasida, (1989)]. [The smallest specimen did produce different tension-softening curves from the other two size specimens, however there were only two data sets for this smallest specimen].

8 REFERENCES

Chong, K.P., K.D. Basham, & D.Q. Wang. 1989. Fracture parameters derived from tension-softening measurements using semi-circular specimens. This volume.

Gopalaratnam, V.S. & S.P. Shah, 1985. Softening response of concrete in direct tension, J. Amer. Concrete Inst. 82:310.

Hashida, T. 1989. Tension-softening curve measurements for fracture toughness determination in granite. This volume.

Hillerborg, A. 1983. Analysis of one single crack. In F. H. Wittmann (ed.), Fracture mechanics of concrete, p.223-250. The Netherlands:Elsevier.

Horvath, R., T. Persson 1984. The influence of the size of the specimen on the fracture energy of concrete. Div. of Building Materials, Lund Institute of Technology, Sweden. Report TVBM-5005.

Li, V.C. 1985. Fracture resistance parameters for cementitious materials and their experimental determination. In S.P.Shah (ed.), Application of fracture mechanics to cementitious composites, p.432. Dordrect:Marinus Nijhoff Publishers.

Li, V.C., C.M. Chan, & C.K.Y. Leung. 1987. Experimental determination of the tension softening relations for cementitious composites, Cement and Concrete Research. 17:441-452.

Leung, C.K.Y. & V.C. Li 1988. Determination of fracture toughness parameter of quasi-brittle materials with laboratory-size specimens. In Press J. of Materials Science.

Petersson, P.E. 1981. Crack growth and development of fracture zone in plain concrete and similar materials. Div. of Building Materials, Lund Institute of Technology, Sweden. Report TVBM-1006.

Reinhardt, H.W. 1984. Fracture mechanics of an elastic softening material like concrete. Heron, Delft University of Technology, 29:2.

Reyes, O.M.L. 1987. Numerical modelling of fracture propagation in tension softening materials, M.S. Thesis, MIT, Cambridge, MA.

Rice, J.R. 1968a. A path independent integral and the approximate analysis of strain concentrations by notches and cracks, J. Applied Mechanics. 35:379-386.

Rice, J.R. 1968b. Mathematical analysis in the mechanics of fracture. In G.C. Sih & H. Liebowitz (eds.), Fracture: an advanced treatise. Vol. 2, p. 191. New York:Academic Press.

Ward, R.J., K. Yamanobe, V.C. Li, & S. Backer 1988. Fracture resistance of acrylic fiber reinforced mortar in shear and flexure. Accepted for publication in Li, V.C. & Z. Bazant (eds.) J. Amer. Concrete Inst.-Sp.Ed.